

## AN EXPERIMENTAL STUDY OF THE CONTRIBUTION OF THE PORE VOLUME CHANGE TO PRODUCTION WITHIN THE FRAMEWORK OF BIOT'S THEORY.

M.J.BOUTÉCA, D.BARY. IFP.  
V.MAURY. EAP.

### ABSTRACT.

The influence of the pore pressure on the elastic strain of rocks is basic to reservoir engineering and environment studies. This paper defines an effective stress law for pore volume variation and presents experimental data to confirm the theoretical framework of poroelasticity while focusing on pore volume variation. For carbonates having porosities in the 4 - 45 % range the effective stress coefficient for the pore volume variation is close to 1. The compressibility of the rock contributes to the total compressibility - i.e. rock + fluid - It is shown that the contribution increases with porosity from 20 - 30 % to more than 100 %.

### INTRODUCTION.

Since 1988 the poroelastic properties of sedimentary rocks have been measured in the IFP lab. A systematic study has been undertaken on carbonates of porosities ranging from 4 % to 45 %. The obtained results are presented to illustrate the contribution of the elastic rock deformation to production and experimentally check Biot's theory.

This paper is divided into 4 parts. In the first part, we briefly summarize the essential features of poroelasticity and define an effective stress law for the pore volume variation. In the second part, we describe the experimental set up and procedure. In the third part, we check the theory previously explained, comparing the computed and measured pore volume variations. In the last part, we compare the pore volume variation to the total fluid volume variation - i.e.pore volume change + fluid compressibility.

### THEORETICAL FRAMEWORK.

Within a reservoir an element of rock may undergo stress variations and pore pressure variations due to the production or due to the fluid injection. In turn those stresses and pore pressure changes induce rock deformation. Depending on the problem with which the reservoir engineer is dealing, he will consider strains (bulk volume changes) or pore volume changes. As a matter of fact if one needs to estimate the reservoir compaction, he only needs to consider strains. On the other hand if one is only considering production then he only needs to consider pore volume changes. Since rock mechanics deals with the relationship between stresses and strains we will state the basic equations which directly answer the bulk changes problem. The corresponding theoretical framework was developed by Biot in 1941 [1] and was also recently reformulated by O. Coussy [2]. We will then derive the equations in terms of pore volume changes which are more familiar to the reservoir engineer. From this result we will illustrate the potential contribution of the elastic rock deformation to oil production. The basic equations which give the relationship between stresses, strains and pore pressure variations are :

$$\partial\sigma_{ij} = \left( K_d - \frac{2G}{3} \right) \partial\varepsilon_{kk} \delta_{ij} + 2 G \partial\varepsilon_{ij} - b \partial P_p \delta_{ij} \quad (1)$$

$$\frac{\partial P_p}{M} = -b \partial\varepsilon_{kk} + \frac{\partial m}{\rho_{ofl}} \quad (2)$$

$\sigma_{ij}$  is the stress tensor,  $\varepsilon_{ij}$  is the strain tensor,  $K_d$  is the bulk modulus,  $G$  is the shear modulus,  $P_p$  is the pore pressure,  $m$  is the fluid mass,  $\rho_{ofl}$  is the fluid density and  $b$  is the Biot coefficient.  $\delta_{ij}$  is Dirac operator ( $\delta_{ij} = 1$  if  $i=j$  and  $0$  if  $i \neq j$ ). We will also make use of the following relationships :

$$b = 1 - \frac{K_d}{K_s} \quad (3)$$

$$\frac{\partial m}{\rho_{ofl}} = \phi c_{fl} \partial P_p + \frac{\partial V_p}{V_b} \quad (4)$$

$$\frac{1}{M} = \Phi c_{fl} + \frac{b - \Phi}{K_s} \quad (5)$$

$K_s$  is the matrix incompressibility modulus i.e. inverse of the matrix compressibility,  $V_p$  is the pore volume,  $V_b$  the bulk volume,  $\Phi$  the porosity,  $c_{fl}$  the fluid compressibility and  $M$  is the Biot modulus.

Note that Eqs(1) and (2) assume a macroscopic scale of homogeneity while Eq(3) assumes a microscopic scale of homogeneity.

In order to underline the physical meaning of Eqs(1) and (2) let us consider lab conditions where the core is placed within a cell under isotropic confining conditions. The pore pressure is allowed to change. Furthermore, we will write the Eqs(1) and (2) in terms of volumes variations instead of strains. Noting that  $\partial\sigma_{kk}/3 = -\partial P_c$ . Eq(1) may be written :

$$-\partial P_c = K_d \frac{\partial V_b}{V_b} - b \partial P_p \quad (6)$$

and Eq(2), making use of (5), gives :

$$\partial P_p \left[ \frac{1}{M} - \Phi c_{fl} \right] = -b \frac{\partial V_b}{V_b} + \frac{\partial V_p}{V_b} \quad (7)$$

Then if the pore pressure is constant Eq(6) clearly shows that  $K_d$  is the inverse of rock compressibility since we get :

$$\frac{1}{K_d} = - \frac{1}{V_b} \frac{\partial V_b}{\partial P_c} \Big|_{\partial P_p=0} \quad (8)$$

For, the same condition ( $\partial P_p = 0$ ), Eq (7) shows a physical meaning of  $b$ . Since from Eq(7) we obtain

$$b = \left. \frac{\partial V_p}{\partial V b} \right|_{\partial P_p = 0} \quad (9)$$

In fact we make use of Eq(8) and Eq(9) in our lab experiments to determine  $K_d$  and  $b$ . Eq(9) gives the physical meaning of  $b$  in terms of volume changes. An other physical meaning can be obtained by rewriting Eq(1) as :

$$\partial \sigma_{ij} + b \partial P_p \delta_{ij} = \left( K_d - \frac{2G}{3} \right) \partial \varepsilon_{kk} \delta_{ij} + 2G \partial \varepsilon_{ij} \quad (10)$$

On the left hand side of the equation, one recognizes the so-called effective stress ( $\sigma_{ij} + b P_p \delta_{ij}$ ).

We will now establish the relationship between the pore volume variation, stress variation and pore pressure variation from Eq(1) through (5). From Eqs (2) and (4) one may see that the pore volume change only depends on the isotropic part of the stress tensor. In other words, for an elastic body, the shearing stress gives no volumetric changes. Hence we may write (1) as :

$$\frac{\partial \sigma_{kk}}{3} = K_d \partial \varepsilon_{kk} - b \partial P_p \quad (11)$$

Introducing Eq(2) and making use of Eqs(3) and (5) leads to :

$$\frac{\partial \sigma_{kk}}{3} = \frac{K_d}{b} \frac{\partial V_p}{V b} - \partial P_p \left[ 1 - \Phi \frac{K_d}{K_s - K_d} \right] \quad (12)$$

One may write (12) as :

$$\frac{\partial \sigma_{kk}}{3} + \alpha_p \partial P_p = K_p \frac{\partial V_p}{V b} \quad (13)$$

$$\text{with } \alpha_p = 1 - \Phi \frac{K_d}{K_s - K_d} = 1 - \Phi \left[ \frac{1}{b} - 1 \right] \quad \text{and } K_p = \frac{K_d}{b} \quad (14)$$

Note that Eq(13) can be considered as an effective stress law for the pore volume variation with  $\alpha_p$  being the pore volume coefficient. One should however remind that the Biot coefficient  $b$  is still included on the right hand side of Eq (13). In other words the effective stress law for the pore volume implies the definition of a pore volume incompressibility  $K_p$  equal to the ratio of  $K_d$  to  $b$ .

We have been measuring  $b$  for carbonates with porosity ranging in the 4% - 45 % range. In table 1 we show these values together with  $\alpha_p$  values. On the whole range of porosities  $\alpha_p$  is roughly constant and equal to 1.

	$\Phi$	$b$	$\alpha_p$
<b>Larrys</b>	0.042 - 0.044	$0.36 \pm 0.06$	0.92
<b>Tavel</b>	0.99 - 0.102	$0.66 \pm 0.04$	0.94
<b>Vilhonneur</b>	0.131 - 0.148	$0.68 \pm 0.04$	0.94
<b>Lavoux</b>	0.233 - 0.239	$0.83 \pm 0.05$	0.94
<b>Estailades</b>	0.289	$0.88 \pm 0.02$	0.96
<b>Meudon</b>	0.448	$0.96 \pm 0.01$	0.98

[Table 1 : Carbonates - poroelastic parameters]

The fact that  $\alpha_p$  is more or less equal to 1 has an important practical application. It means that any measurement of pore volume variation may be performed either by increasing the external volumetric stresses or by decreasing the pressure. The stress increase  $\partial\sigma_{kk}/3$  ( $= -\partial P_c$  for a test with isotropic confining stress) is equal to the pore pressure decrease.

## EXPERIMENTAL STUDY OF THE THEORETICAL FRAMEWORK.

A detailed description of the experimental set-up, of the procedure and of the estimation of the experimental error are given in a previous paper (Laurent, 1993) [3].

## EXPERIMENTAL SET-UP.

The experimental set-up consists of a pressure cell and two volumetric pumps. The sample is coated with impermeable materials which allow application of pore pressure and confining isotropic pressure. One volumetric pump is connected to the confining fluid and the other one communicates with the pore through a micro well (Fig. 1). The use of small tubings and low injection volumes reduces errors induced by the compressibility of the system to a minimum. The sample is 5 cm in diameter and 14 cm long. The volumetric pumps have a maximum pressure of 200 MPa. Core coating is made of two layers : a very thin impermeable metallic coating is sprayed on the surface and 0.05 cm thick coating of epoxy resin provides mechanical protection.

## EXPERIMENTAL PROCEDURE.

The four variables  $P_p$ ,  $P_c$ ,  $V_b$ ,  $V_p$  are measured or controlled independently and simultaneously. The volumetric pumps coupled with pressure gauges are used to control and measure the confining pressure and the bulk volume on one side and the pore pressure and the pore volume on the other side. The sample is saturated in the cell first in a vacuum, then circulating. To avoid accumulation of micro leaks at different connections of the apparatus and to minimise creep phenomena in the sample, every experiment is completed within 12 hours. The same protocol is used for all the samples (Fig.2). The confining pressure is increased first while a constant pore pressure is maintained. A constant confining pressure is then maintained while the pore pressure is increased. To ensure a good coating contact the minimum difference between confining pressure and pore pressure is 2 MPa. After several cycles of pressure increases, we

decrease the pressures by the same procedure. With high porosity rocks (more than 15 %), we could obtain at least 50 measurement points per experiment. But with lower porosity rocks (5%), steady values for pore pressure were obtained only after at least 30 minutes and only 15 measurements points were recorded. In figures 3 to 7 we represent the pressure domain explored by plotting confining pressures versus corresponding pore pressures.

#### PORE VOLUME VARIATION : THEORY V.S. EXPERIMENT.

One may readily compute the pore volume variation from Eq (13) :

$$\partial V_p = V_b \left[ \frac{b}{K_d} \frac{\partial \sigma_{kk}}{3} + \left[ \frac{b - \Phi + b\Phi}{K_d} \right] \partial P_p \right] \quad (15)$$

To check the theory herein explained with reference to the reservoir engineering problems, we plotted the pore volume variation computed from Eq (15) versus the measured pore volume variation. The 5 limestones (more than 98 % calcium carbonate) and the chalk corresponding to 6 porosities are the Larrys - moucheté limestone ( $\Phi=4.5\%$ ), the Tavel limestone ( $\Phi=10\%$ ), the Vilhonneur limestone ( $\Phi=14\%$ ), the Lavoux limestone ( $\Phi=24\%$ ), the Estailades limestone ( $\Phi=29\%$ ) and the Meudon chalk ( $\Phi=45\%$ ). The obtained results are shown for the Larrys, Tavel and Vilhonneur limestones respectively on Fig.8, 9 and 10. Figures 8 and 9 show an excellent agreement between the computed and experimental values of the pore volume variation (the slope 1 curve is shown). In fact though  $b$  and  $K_d$  vary slightly with both pressure and confining stress, the overall effect still leads to a linear relationship between the pore volume variation and the "pore volume effective stress" (see Eq (13) for instance). Furthermore for the Larrys limestone 2 different samples (LMA, LMB) were studied and 2 different samples were also studied for the Tavel (Tavel A, Tavel C) limestone. In both cases we used the same  $b$  and the same  $K_d$  for both samples while computing the pore volume variation. For Larrys limestone, the confining pressure was increased up to 52 MPa and the pore pressure was increased up to 50 MPa (see Fig.3). For the Tavel limestone the confining pressure was increased up to 98 MPa while the pore pressure was increased up to 72 MPa (see Fig.4). In Fig. 10 the results are shown for one of the tests. the points show a clear trend parallel to the slope 1 curve but the computed values seem to be under-estimated. In order to better understand we represented in Fig.11 the computed values in a dashed line and the experimental values in a solid line versus time. The loading and unloading cycles were symmetrical and similar to the one shown on Fig 2. The confining pressure was increased from 2 MPa up to 36 MPa and the pore pressure was increased from 2 MPa up to 26 MPa. In Fig.11 one may observe that the experimental pore volume variation does not go back to 0 though the loading/unloading cycles are symmetrical. Two phenomena may be suspected : (a) plasticity of the rock and (b) fitting of the coating on the rock. Experiment B3 was the third experiment and B1 and B2 had been conducted under the same level of stresses. Hence if it were plasticity, experiments B2 and B3 would not show a plastic deformation. We thus considered it as a fitting of the coating on the rock which should take place during the first loading cycle. We thus shifted the computed curve in such a way that at the end of the first loading (point A) the shifted computed curve is at the same value than the experimental one. The shifted curve is represented in a dotted line. Thus the shifted line is under the experimental one during the fitting phase and then the shifted and experimental are identical. Since the same fitting problem was observed on the more porous samples we represented the results in the same way on Fig.12 and 13. For the experiment LD (Fig.12) (Lavoux limestone) the confining pressure was increased up to 36 MPa and the pore pressure was increased up to 26 MPa. For the experiment ESTA1 (Fig13 - Estailades limestone), the confining pressure was increased up to 34 MPa and the pore pressure was increased up to 25 MPa. the shift due to the fitting of the coating is higher but the shifted curve and the experimental one are close to each other afterwards. On Fig.13 one can see clearly the effect of the coating. When the pore pressure nears

the confining pressure (point B for instance) the experimental curve moves away from the translated curve. When confining pressure is increased the two curves come together (point C). This phenomenon indicates a fluttering of the membrane governed along the surface porosity by the difference between the outside pressure (confining) and inside pressure (pore).

### "PORE COMPRESSIBILITY" AND FLUID COMPRESSIBILITY.

Let us consider Eq(13). Since  $V_p = \Phi V_b$ , it may be written :

$$\frac{\partial V_p}{V_p} = \left[ \frac{1-b}{\Phi K_d} \right] \frac{\partial \sigma_{kk}}{3} + \left[ \frac{1-b-\Phi+b\Phi}{\Phi K_d} \right] \partial P_p \quad (16)$$

This equation has to be compared with :

$$\frac{\partial V_f}{V_p} = c_f \partial P_p \quad (17)$$

Comparison between Eqs (16) and (17) shows that in order to define a global compressibility  $C_t$  in reservoir engineering as the sum of the fluid compressibility and the pore compressibility one must be able to define  $\partial \sigma_{kk}$  (i.e. the stress variation) as a function of the pore pressure variation. This can only be done by assuming "boundary conditions" for the mechanical deformation (Boutéca, 1992) [4]. This emphasizes the fact that any rock compressibility measurement in our lab implicitly includes an assumption on the mechanical behaviour of the reservoir. To estimate the rock compressibility influence, let us assume that the reservoir is depleted at constant total stress condition. this corresponds to an experimental condition where the confining pressure is kept constant while the pore pressure changes. Hence from Eq(16) it appears that one will measure  $\left[ \frac{1}{\Phi} \left( \frac{b-\Phi+b\Phi}{K_d} \right) \right] = c_{mp}$  which can be directly compared with  $c_f$ . The comparison is shown on Fig.14 for the fluid used in our experiments (water) in which  $c_f / (c_f + c_{mp})$  is plotted as a function of  $c_{mp}$ . If  $c_{mp}$  were negligible the ratio would be constant and equal to 1. As a matter of fact, for the rocks considered, the ratio varies in the range of 0.8 to 0.5.

### CONCLUSIONS.

1. An effective stress law for the pore volume variation was derived. Our experimental results obtained with carbonates for porosities ranging in the 4 - 45 % range show that the pore pressure coefficient is close to 1. The stiffness which relates the pore volume variation to the effective stress law is equal to the bulk incompressibility divided by the Biot coefficient.
2. Measurements performed on samples of various limestones and one chalk confirm the theoretical framework of the poroelastic theory.
3. Elastic pore volume change contribution to the total compressibility - ie. pore volume + fluid compressibility - increases with porosity from 20 - 30 % to more than 100 %.

## ACKNOWLEDGEMENTS.

The authors would like to express their gratitude to J.P.Sarda and O.Vincké of the Institut Français du Pétrole and D.Fourmaintraux and J.M.Piau of EAP for their useful contribution.

## REFERENCES

- [1]  
Biot, M.A., 1941, "General Theory of Three Dimensional Consolidation, J. Appl.Phys., 15, 155-164.
- [2]  
Coussy, O., 1991, Mécanique des Milieux Poreux, Ed. Technip, Paris.
- [3]  
Laurent, J., Boutéca, M.J., Sarda, J.P. and Bary, D., 1993, "Pore-Pressure Influence in the Poroelastic Behaviour of Rocks : Experimental Studies and Results, SPEFE, june 1993, SPE 20922.
- [4]  
Boutéca, M.J., 1992, "Elements of Poroelasticity for Reservoir Engineering", Revue de l'Institut Français du Pétrole, Vol.47, n°4, 479-490.

## NOMENCLATURE

Kd	bulk modulus
G	shear modulus
Pp	pore pressure
Pc	confining pressure
m	fluid mass
Ks	matrix incompressibility modulus
$\sigma_{ij}$	stress tensor
$\epsilon_{ij}$	strain tensor
$\phi$	porosity
b	Biot's coefficient
c <sub>fl</sub>	fluid compressibility
M	Biot's modulus
V <sub>p</sub>	pore volume
V <sub>b</sub>	bulk volume
V <sub>fl</sub>	fluid volume

Fig. 1 : EXPERIMENTAL SET-UP

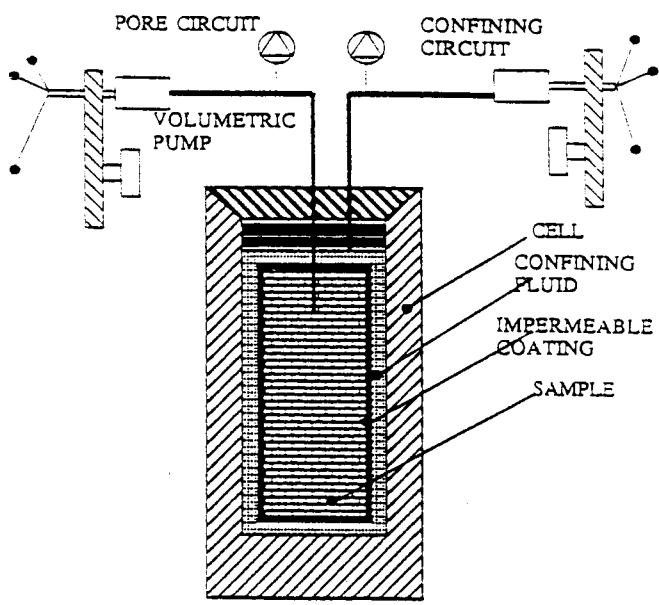


Fig. 2 : EXPERIMENTAL PROTOCOL

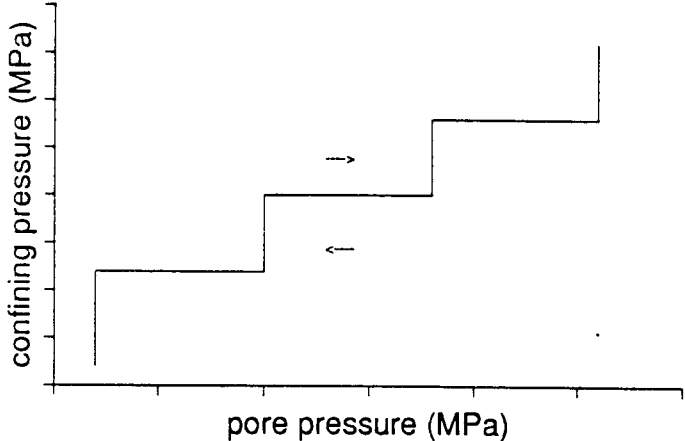


Fig. 3 : Larrys limestone - pressure domain

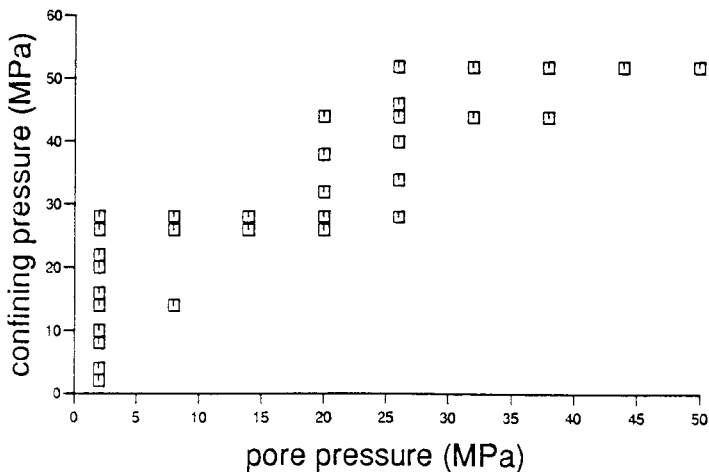




Fig. 4 : Tavel limestone - pressure domain

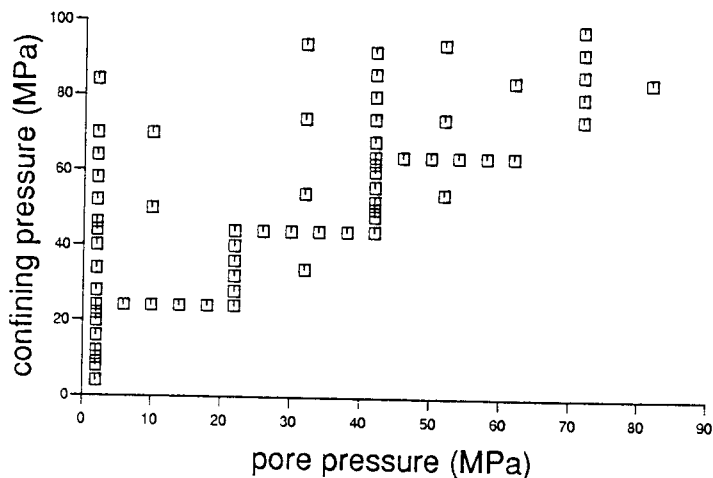


Fig. 5 : Vilhonneur limestone - pressure domain

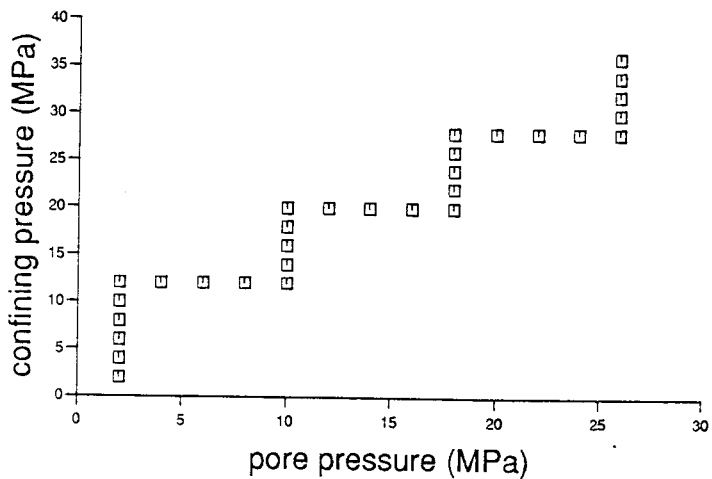


Fig. 6 : Lavoux limestone - pressure domain

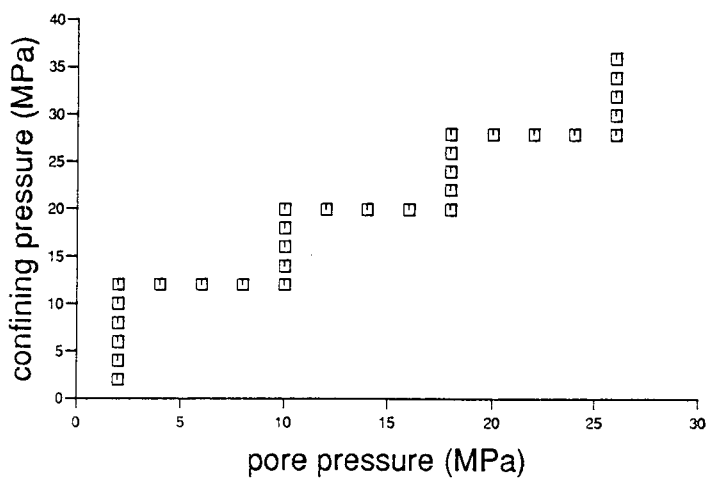


Fig 7 : Estailades limestone - pressure domain

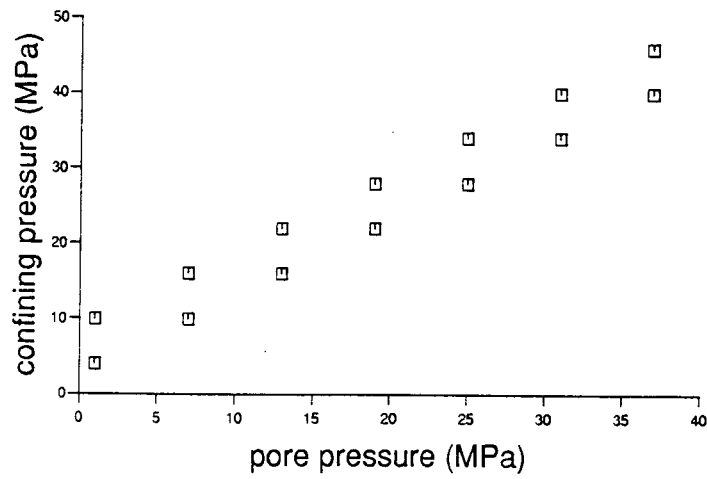


Fig. 8 : LARRYS limestone - pore volume variation

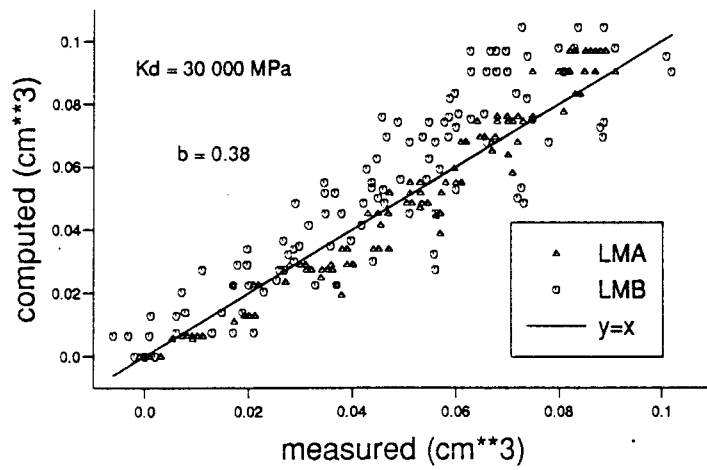


Fig. 9: TAVEL limestone - pore volume variation

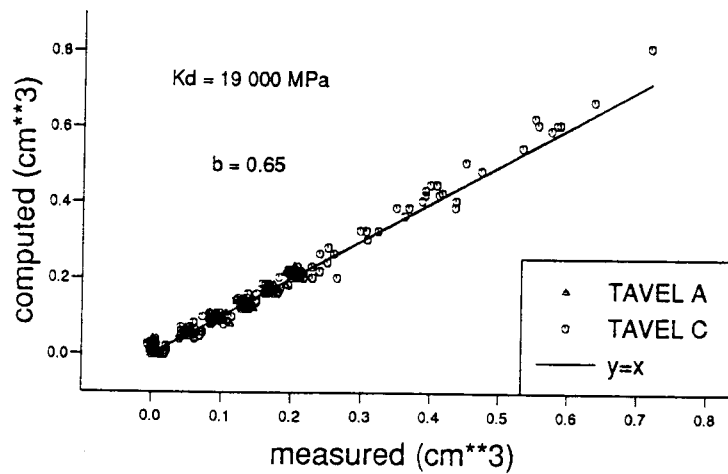


Fig. 10: VILHONNEUR limestone - pore volume variation

$K_d = 20\ 000\ \text{MPa}$   $b = 0.7$

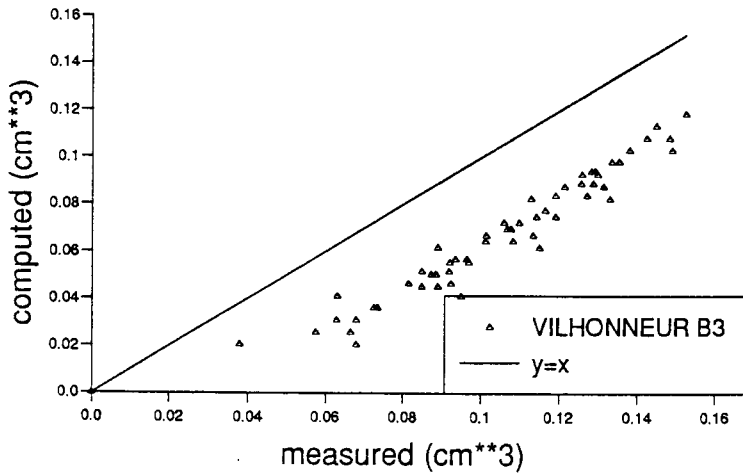


Fig. 11 : VILHONNEUR limestone - pore volume variation

$K_d = 20\ 000\ \text{MPa}$   $b = 0.7$

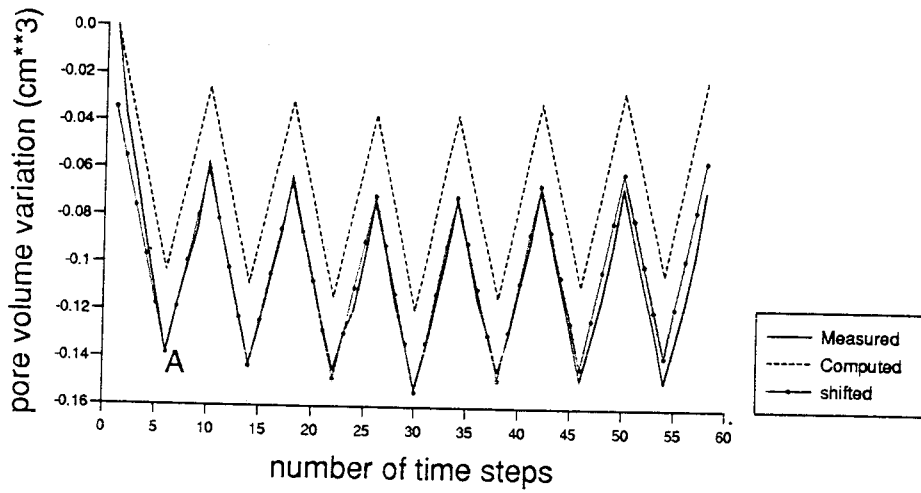


Fig. 12 : LAVOUX limestone - pore volume variation

$K_d = 9500\ \text{MPa}$   $b = 0.82$

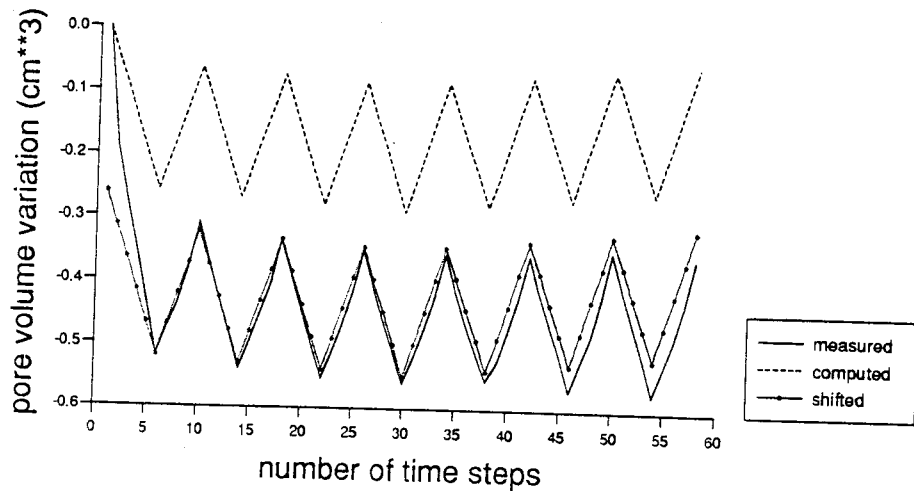


Fig. 13 : ESTAILLADES limestone - pore volume variation  
 $K_d = 6500 \text{ MPa}$   $b = 0.9$

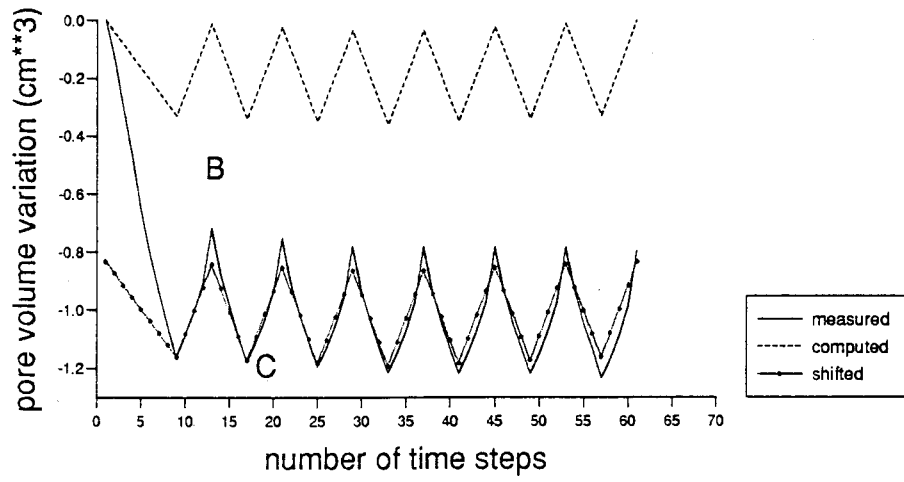


Fig. 14 : INFLUENCE OF ROCK COMPRESSIBILITY

